Check for updates

One-pot synthesis of self-healable and recyclable ionogels based on polyamidoamine (PAMAM) dendrimers via Schiff base reaction†

Xiaomeng Zhao, Shufei Guo, Hao Li, Jiahang Liu, Cuiping Su and Hongzan Song [iD] *

Novel ionogels with covalent polymeric networks based on polyamidoamine (PAMAM) dendrimers have been synthesized by the *in situ* crosslinking of amines *via* Schiff base reaction in the ionic liquid 1-ethyl-3-methylimidazolium acetate ([EMIM][OAc]). The obtained ionogels have excellent self-healing ability and recyclability. Rheological measurements revealed that the plateau modulus in storage modulus increases with increasing dendrimer content, and increasing generation of dendrimers results in the decrease of the plateau modulus due to geometrical reasons. The ionogels are very stable, and the reversible covalent networks are not destroyed at temperatures up to 160 °C, as indicated by dynamic temperature sweep measurements. Remarkably, the ionogels exhibit high ionic conductivity, and room-temperature ionic conductivity can reach 10^{-2} S cm^{-1}. These self-healable and recyclable ionogels with high conductivity, good mechanical properties, and easy processability are desirable for flexible electronic devices with superior lifespans.

Introduction

Ionogels, unique hybrid materials in which ionic liquids (ILs) are immobilized in a three-dimensional network, have attracted tremendous attention and shown promising applications in various electrochemical devices.[1–5] Particularly, ionogels are emerging as the main building blocks for flexible devices due to their high conductivity, safety and flexibility.[6–10] However, ionogels break under the complex deformations that often occur during use (*e.g.*, bending, rolling and twisting), leading to irreversible damage. The resulting loss of structural integrity leads to the degradation of mechanical and electrochemical performance or even serious safety problems. Therefore, it is both desirable and challenging to solve the breakage problem and prolong the service life of ionogels.[11–15]

Self-healing, which refers to the ability of biological and artificial systems to spontaneously repair damages and restore function, has attracted much attention from researchers and inspired them to explore self-healing materials.[16–20] Among these materials, dynamic polymeric materials are the most studied due to the automatic and intrinsic healing nature of the polymers, their relative ease of modification, and their wide applicability.[21] In general, two approaches based on dynamic covalent bonds and noncovalent bonds have been developed to obtain dynamic polymeric materials.[13,21–24] The

first route uses dynamic covalent chemistry based on the thermodynamic equilibrium between bond dissociation and restructuring.[25–31] The second method is based on noncovalent interactions, including hydrogen-bonding, $\pi-\pi$ stacking, charge transfer, and hydrophobic interactions.[32–38] However, noncovalent bonding systems are often unstable and do not have sufficient mechanical strength. Conversely, dynamic covalent bonding systems containing reversible but strong covalent bonds are desirable for polymeric materials with healable structures. By far, research about self-healing ionogels is rarely reported and only exits in biopolymer/ionic liquid systems through noncovalent interactions with low mechanical strength.[39,40] Thus, it is desirable to prepare self-healing ionogels involving reversible covalent bonds with high mechanical strength and good electrochemical properties.

Dendrimers, a unique class of macromolecules with uniform, repeating branching units, have received considerable attention due to their unique chemical and physical properties as well as their potential applications in biomedical science, environmental science, and materials science.[41–44] Dendrimers are completely amorphous with many cavities in their internal structures. They also have large numbers of branch ends with high segmental motion, makes them attractive as hosts for polymer electrolytes.[45,46] More importantly, the abundant functional groups in the molecular structures of dendrimers allow them to easily form dynamic covalent bonds or noncovalent bonds, resulting in excellent self-healing ability.[47–51] Therefore, their unique branched architectures and physicochemical properties make dendrimers an exciting choice for preparing

College of Chemistry & Environmental Science, Hebei University, Baoding, Hebei Province 071002, P. R. China. E-mail: songhongzan@iccas.ac.cn

self-healing ionogels with high ionic conductivity and good mechanical properties.

Herein, novel self-healing ionogels based on polyamido-amine (PAMAM) dendrimers are presented for the first time, to the best of our knowledge. The ionogels were prepared by *in situ* amines crosslinking *via* the Schiff base reaction in ionic liquid. The reversible covalent crosslinks can endow the ionogel with highly-efficient self-recovering ability that without external stimuli. We also report the effects of polymer concentration, temperature, dendrimer generation and water content on the viscoelasticity and ionic conductivity of the ionogels.

Experimental methods

Materials

PAMAM dendrimers, ethylenediamine cores, and generation G0-5 solutions (20 wt% in methanol) were purchased from Sigma-Aldrich and used after removal of methanol (the M_w and the number of terminal amino groups for different generation PAMAM are shown in Table S1 in the ESI).† Methylglyoxal was purchased from Sigma-Aldrich and used as received. The ionic liquid 1-ethyl-3-methylimidazolium acetate ([EMIM][OAc]) was purchased from Sigma-Aldrich. The ionic liquid was dried at 80 °C under vacuum for 24 h prior to use, and the water content measured by Karl Fischer titration was 0.05 wt%.

Preparation of self-healing ionogels

Cross-linked polymeric gels were prepared by dissolving PAMAM (generation G1–5) in ionic liquid with slight heating and allowing the solution to cool to 0 °C in an ice-water bath before adding methylglyoxal. The initial stoichiometric ratios between methylglyoxal and amine functional groups were kept at unity for all reactions to ensure 50% functional group conversion. Note that the initial concentrations of the [methylglyoxal] and [amine] functional groups were kept at 0.5 M. A representative procedure is given as follows. PAMAM G1 (0.6 g, 0.42 mmol) was dissolved in 0.7 g of [EMIM][OAc] at 40 °C under stirring for 1 h and then cooled to 0 °C in an ice-water bath. Methylglyoxal (129 μL, 0.84 mmol) was also dissolved in 0.7 g [EMIM][OAc] at ambient temperature and then cooled to 0 °C in an ice-water bath. The above solutions were mixed under stirring in an ice-water bath. After the solution became homogeneous, it was slowly transferred to a mold using a pipette to minimize the formation of air bubbles. The mold was covered with two parallel plates at the top and bottom. The mixtures were allowed to stand in the mold at room temperature for 2 h, after which the self-healing ionogel with 30% PAMAM G1 was obtained. The water content of this ionogel measured by Karl Fischer titration was 5 wt%. The structures of the used raw materials and the reaction scheme are shown in Fig. 1. Note that the Schiff base reaction is a reversible reaction, and the only byproduct is water; thus, the self-healing ionogels contain small amounts of water (1–5 wt%).
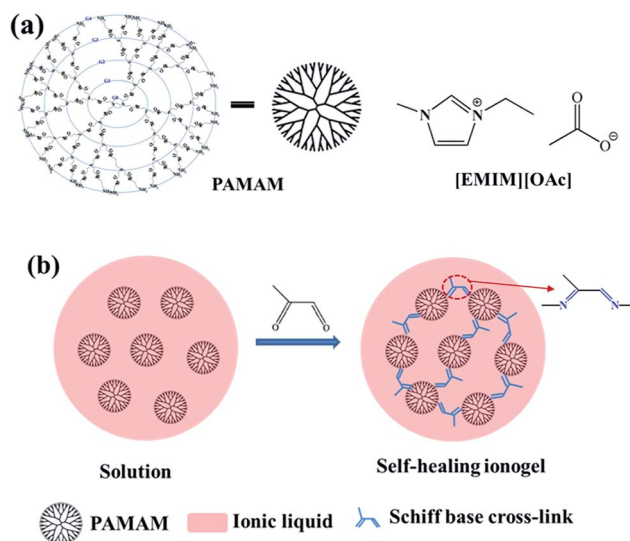

Fig. 1 (a) Chemical structures of PAMAM and [EMIM][OAc]. (b) Schematic illustration of the synthetic process and structure of the self-healing ionogel.

Characterization

Scanning electron microscopy (SEM) images of the samples were obtained on a JEOL SEM 6700 microscope operating at 5 kV. The ionogel samples were surface-treated and coated with platinum before SEM observation. Optical micrographs were obtained using a BX51 Olympus polarized optical microscope (Olympus, Japan). Mechanical properties were studied using a Linkam LINKSYS 32 tensile hot stage (Linkam, UK), at room temperature at a rate of 0.2 mm min⁻¹. Rheological measurements were performed on a stress-controlled rheometer (TA-AR2000EX, TA Instruments) with a parallel-plate geometry (diameter = 25 mm). Before oscillatory shear measurements, a strain sweep from 0.1% to 100% with a fixed frequency of 6.28 rad s⁻¹ was performed for each sample to determine the linear viscoelastic regime. The chosen strains of 1–10% fell well within the linear viscoelastic regime for the frequency range of 0.01–100 rad s⁻¹ in the oscillatory shear measurement. The experimental temperature was mainly set at 25 °C. Dynamic temperature sweep measurements at an angular frequency of 6.28 rad s⁻¹ were conducted from 25 °C to 200 °C with a heating rate of 1 °C min⁻¹. For each sweep measurement, three specimens were analyzed to assess data reproducibility. All measurements were conducted under nitrogen atmosphere. Thermal analysis of the ionogels was performed using a Perkin-Elmer TGA 6 instrument (PerkinElmer Instruments, USA). The temperature ranged from 40 °C to 800 °C with a heating rate of 15 °C min⁻¹ under nitrogen. The ionic conductivities of the self-healing ionogels were measured using a Zahner IM6e electro-chemical workstation (Zahner, Germany) over the frequency range of 1 Hz to 500 kHz at an AC oscillation of 10 mV. All measurements were conducted under nitrogen atmosphere. The samples (diameter = 8 mm, thickness = 2 mm) were measured in a cell that consisted of a Teflon spacer sandwiched between two platinum-coated stainless-steel electrodes. The cell

constant was determined using a 0.01 M KCl aqueous solution at 25 °C as the reference. Ionic conductivities were calculated from the bulk resistances obtained from the impedance spectra. The minimum in the Nyquist plot of the negative imaginary part of impedance *versus* the real part of impedance was taken as the sample resistance, R. The ionic conductivity, σ, was calculated as $\sigma = d/(RS)$, where d and S are the thickness and area of the sample, respectively. FTIR spectra were recorded in the region of 400–4000 cm^{-1} for each sample on a Varian-640 spectrophotometer. The spectrum for each sample was obtained by averaging 32 scans over the selected wavenumber range. Liquid-state and solid-state ^{13}C CP/MASS NMR spectra were obtained on a Bruker Advance III spectrometer. The samples were spun at 8 kHz. A contact time of 4 ms, repetition time of 12 s, and spectral width of 24 kHz were used for the total of 1000 scans.

Results and discussion

Synthesis and characterization of self-healing ionogels

Dynamic covalent polymeric networks composed of imine linkages were prepared *via* Schiff base reaction from PAMAM dendrimers and methylglyoxal in [EMIM][OAc] (Fig. 1). Taking into consideration the special topological structure of the PAMAM dendrimers and the volume shrinkage upon cross-linking, the initial concentrations of the [aldehyde] and [amine] functional groups were both kept at 0.5 M. The ^{13}C NMR spectra were used to confirm the formation of C=N bonds, and the results are illustrated in Fig. S1 and S2.† The appearance of a peak at $\delta = 164.51$ ppm assigned to the C=N group confirmed the Schiff base reaction.[30,52] In addition, the functionalization was confirmed by comparing the FTIR spectra of pure PAMAM, [EMIM][OAc] and the ionogels (Fig. S3†). For PAMAM, the characteristic band of –NH$_2$ displays at 3277 cm^{-1}, the N–H is present at 1542 cm^{-1}, and the C=O stretching band is found at 1635 cm^{-1}. In the ionogel spectrum, the distinct band corresponding to –NH$_2$ groups at 3277 cm^{-1} is decreased by approximately 50% compared to in the spectrum of PAMAM, indicating that aldehyde is almost quantitatively converted. Large shifts in wavenumber from 1631 to 1650 cm^{-1} (overlap of the C=N vibration with the C=O vibration of cross-linked PAMAM) and from 1542 to 1556 cm^{-1} (O=C–N–H stretching) indicate strong interactions between the ionic liquid and PAMAM skeleton.[53,54]

Ionogel microstructures

The ionogels obtained with ionic liquid [EMIM][OAc] are transparent and easy to process into any shape. Fig. 2a shows a photo of a round-shaped self-healing ionogel. Noticeably, the obtained ionogels possess good self-supporting performance and can be bent, demonstrating the good mechanical properties of the ionogels (Fig. 2b). To study the morphologies and microstructures of the ionogels in detail, the ionogels were investigated by SEM. Note that the samples were surface-treated using acetone before SEM observation, which could clean up the ionic liquid and produce gentle etch to observe the architecture more directly and clearly. For the ionogels without
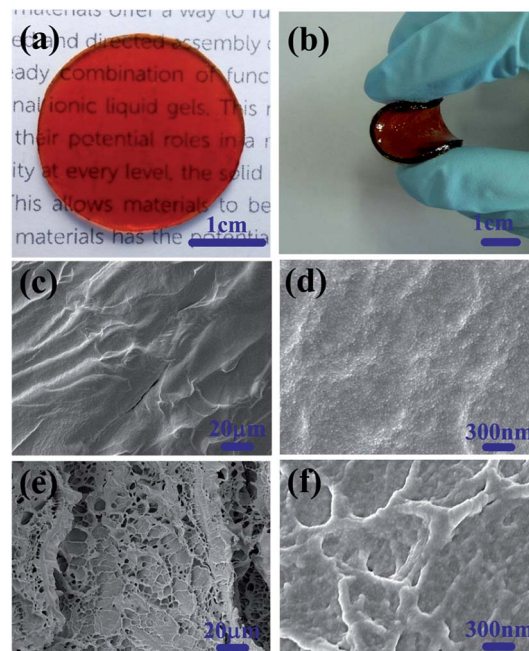

Fig. 2 Ionogel morphology and structure: (a) round-shaped ionogel; (b) bent round-shaped ionogel; and SEM images of (c) and (d) ionogel cross sections (e) and (f) surface-treated ionogel cross sections.

surface treatment, the cross-sectional surface is rough with numerous PAMAM spherules (Fig. 2c and d). After surface treatment, ubiquitous porous microstructures with pore diameters of 5–12 μm were observed. Fig. 2f shows an enlarged SEM image of the pore wall. The pore wall has a network structure constructed from numerous uniform, spherulitic and cross-linked particles (Fig. 2e and f).

Self-healing properties of ionogels

As shown in Fig. 3a–d and the optical images (Fig. S4†), the severed ionogel (20% PAMAM G1) sample recombined in short time period without any stimulus. This excellent self-healing property can be explained as follows (Fig. 3e). The self-healing of the ionogel is driven by the dynamic reversible exchange of Schiff base bonds. The crosslinking of carbon–nitrogen double bonds is a critical structural factor that contributes to the dynamic characteristics and complete reaction between aldehyde and amine. These PAMAM-based ionogels contain many more amines per molecule than other ionogels based on linear molecules, resulting in quick and repeatable self-healing without any external stimulus at room temperature. Furthermore, the abundant amine groups in the PAMAM backbone produce large numbers of carbon–nitrogen double bonds, which mechanically strengthen the ionogels. The self-healing ability of the ionogels is more clearly illustrated in Fig. 3f by the stress–strain curves of the repaired samples. For the original self-healing ionogels, the tensile strength and elongation at break are 48.2 kPa and 36.5%, respectively. When the healing time was 30 minutes, the elongation of the repaired sample can recover 51%. When the severed samples were allowed to repair
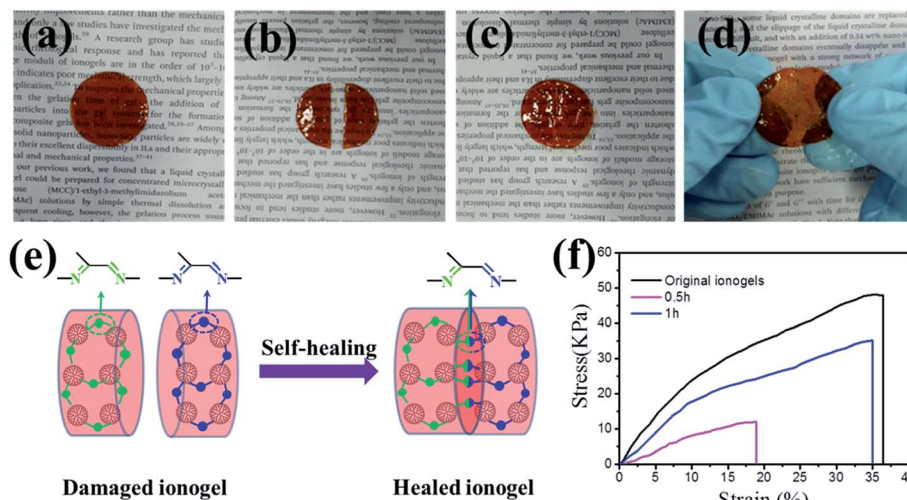
Fig. 3 Self-healing process of the ionogel: (a) original ionogel; (b) ionogel after being cut by a knife; (c) ionogel after contact and then free standing for 1 h; and (d) under drawing for the healed samples. (e) The proposed mechanism of self-healing process, (f) stress–strain curves of original ionogels and ionogels healed for different times.

for 1 hour, the extensibility recovery was 95%, and the recovery in tensile strength was 73%. Note that the destroyed samples can completely recover in about 2 h after contact.

Rheological behaviors of ionogels

To study the dynamic viscoelasticities of the ionogels in detail, rheological measurements were performed. The values of storage modulus, G', loss modulus, G'', and complex viscosity, $|\eta^*|$ as functions of angular frequency, ω, for ionogels with different PAMAM contents at 25 °C are shown in Fig. 4. For the

ionogel with 10% PAMAM G1, G' is always higher than G'', and the moduli are relatively independent of frequency in the explored frequency. The value of $|\eta^*|$ decreases linearly with increasing frequency, suggesting the existence of a gelating network.[55,56] Importantly, for the ionogel with 20% PAMAM G1, in the high-frequency regime, the sample displays a solid-like characteristic with $G' > G''$. In addition, G' is independent of frequency because there is not sufficient time for labile cross-links to dissociate at high frequency and this modulus is referred to as plateaus modulus (G_N), which is an important
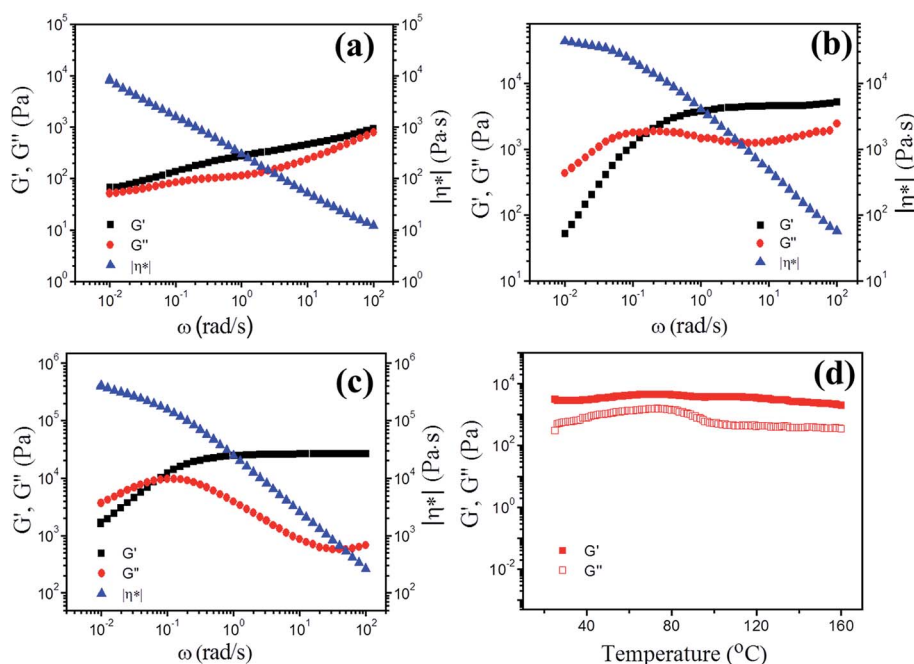

Fig. 4 G', G'', and $|\eta^*|$ as functions of ω at 25 °C for ionogels with different contents of PAMAM G1: (a) 10%, (b) 20%, and (c) 30%. (d) G' and G'' as functions of temperature at an angular frequency of 6.28 rad s^{-1} for ionogel with 20% PAMAM G1.

value to reflect the effective cross-linking density among the gel network; thus, elastic-like behavior dominates. At low frequency, the G'' curve intersects the G' curve at 0.16 rad s^{-1}, and the "terminal region" that the relations of $G'–\omega^2$ and $G''–\omega$ are observed at lower frequencies. The reason is that the time scale probed is longer than the lifetime of the kinetically labile crosslinks, thus allowing time for the network to restructure at lower frequencies. This typical frequency-dependent G' and G'' behavior has been observed for gels containing reversible covalent bonds (*i.e.*, acylhydrazone and disulfide bonds)[28,30,54] and supramolecular networks formed by host–guest interactions (*i.e.*, hydrogen bonding, π–π stacking, and metal–ligand interactions).[33,57–59] The ionogel with 30% PAMAM G1 has similar rheological behavior to the sample with 20% PAMAM G1, and a low-frequency crossover appears at 0.08 rad s^{-1}; however, the sample with 30% PAMAM G1 has a much higher plateau modulus in storage modulus (27 kPa) than the sample with 20% PAMAM G1 (4.7 kPa). Interestingly, the ionogels are very stable over a wide range of temperatures, and the solid-state structure is not destroyed at temperatures up to 160 °C, as confirmed by dynamic temperature sweep measurements (Fig. 4d).

PAMAM generation has been shown to influence the dynamic viscoelasticities of ionogels; increasing dendrimer generation results in the decrease of the plateaus modulus, as revealed by the oscillatory rheological measurements of the ionogels with PAMAM G0–G5 at 25 °C. For example, the sample with 30% PAMAM G1 shows a plateau modulus in storage modulus of about 27 kPa, while that for the sample with 30% PAMAM G4 is 1.2 kPa (Fig. S5†). The ionogel samples with the same total amounts of dendrimers should have approximately the same plateau modulus in storage modulus because they have approximately the same theoretical crosslinking densities according to the equation $G_N = \nu_\chi RT$, where G_N is the plateau modulus, ν_χ is the network density, R is the universal gas constant, and T is the temperature.[60] However, the plateaus modulus for low generations is much higher than that for high generations, indicating that the network density is much higher for low generations than for high generations. This unique behavior might be explained as follows. For higher generations, the topological structure of PAMAM dendrimers becomes close to a molecular spherical architecture, limiting the crosslinking ability *via* geometric constraint.[41,60]

Ionic conductivity of ionogels

Based on the data obtained by impedance spectroscopy measurements (Fig. S6†), the temperature dependencies of the ionic conductivities of neat [EMIM][OAc], ionogels with different contents of PAMAM with the same generation number, and ionogels with the same contents of PAMAM with different generation numbers are shown in Fig. 5. In all cases, the ionic conductivity monotonically increases with increasing temperature. The ionic conductivity decreases with increasing PAMAM G1 content because the decrease in [EMIM][OAc] content with increasing PAMAM content results in the reduction in ion concentration. Furthermore, the ionic conductivity
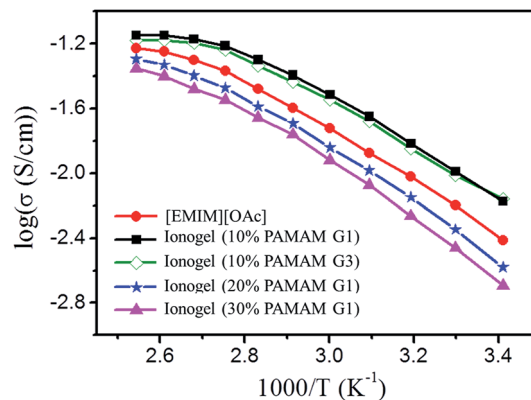

Fig. 5 Temperature dependence of the ionic conductivities of neat [EMIM][OAc] and ionogels shown in the Arrhenius convention.

decreases with increasing PAMAM generation. For example, the sample with 10% PAMAM G3 shows a lower ionic conductivity than the sample with 10% PAMAM G1 at all temperatures investigated. More importantly, the room-temperature ionic conductivities of all the ionogels are higher than 1.0×10^{-3} S cm^{-1}, which meets the requirement for the practical application of gel polymer electrolytes. For example, the ionic conductivity of the ionogel with 10% PAMAM G1 reaches 10^{-2} S cm^{-1} at room temperature, which is higher than that of neat [EMIM][OAc]. According to the literature, the conductivity of the electrolyte depends on the carrier concentration as well as on ionic mobility.[61–63] In our system, the crosslinked PAMAM dendrimers provide conducting pathways for ion transport due to their amorphous nature, abundance of cavities in the internal structure, and large number of branch ends with high segmental motion. Second, and possibly more importantly, the self-healing ionogels contain little water (3 wt%), resulting in increased mobility and hence conductivity.[63] However, when the PAMAM concentration is above 20% (water content about 5 wt%), the decrease in the number density of carrier ions causes the ionic conductivity to fall below that of neat [EMIM][OAc], although the ionic conductivity is still higher than 1.0×10^{-3} S cm^{-1}. Therefore, the as-prepared ionogels with high ionic conductivity and adjustable self-restoring mechanical properties are excellent electrolyte candidates for ideal electrochemical performance.

Effect of water content on ionic conductivity and modulus of ionogels

Water can affect the ionic mobility and structure of the electrolyte, thus affecting the performance of electronic devices.[63–65] The results, thus far, have been mixed. For some liquid-crystalline gel polymer electrolytes[64] or triblock copolymer ionogel systems,[65] water can reduce the structural ordering of the electrolyte, thus negatively affecting the performance. However, in some ionogels based on hygroscopic ionic liquids, water remarkably increases the mobility of the ionic liquid and slightly decreased the modulus, thus positively affecting performance.[63] To investigate this further, different contents of
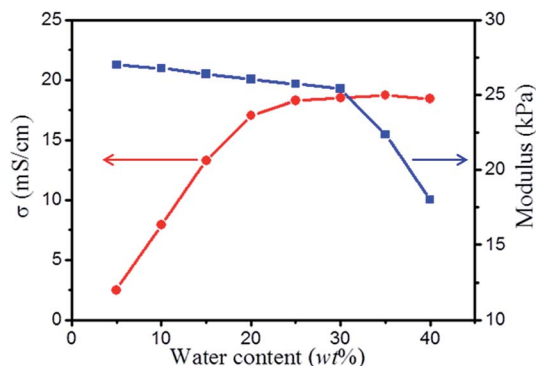
Fig. 6 Ionic conductivities and moduli of ionogels (30% PAMAM G1) with various water contents.

water were added to the ionogels, and the resulting electrochemical and mechanical properties were compared. Fig. 6 presents the plots of ionic conductivity and modulus for the ionogels (30% PAMAM G1) with various water contents. Interestingly, the ionic conductivity significantly increases from 2.5 to 18.2 mS cm^{-1} as the amount of water increases from 5 to 40 wt%. This is because as water is added to the ionogel, the ionic mobility significantly increases.[63] Furthermore, the modulus slightly decreases from 27 to 25.3 kPa as the amount of water increases from 5 to 30 wt% and then decreases sharply from 25.3 to 17.3 kPa as the amount of water increases from 30 to 40 wt%. The possible reason is that when an appropriate amount of water is added, the reversible covalent bonds are barely effected. When excess water is added, some of the reversible covalent bonds are disintegrated, resulting in a decrease in network density. When

the amount of water exceeds 45 wt%, the ionogel changes into a colloidal state without a stable shape.

Recyclability of ionogels

Most chemical crosslinking ionogel electrolytes used in flexible batteries and supercapacitors are crosslinked by common covalent crosslinking bonds; these bonds are hard to break, making the ionogel too difficult to process and reuse.[3,5–7] However, the prepared PAMAM ionogel electrolytes with dynamic covalent bonding are easier to process and recycle. The recyclability of the ionogel electrolyte was studied, as shown in Fig. 7. Fig. 7a–f schematically show how the PAMAM ionogel with intact round shape gradually turned into a liquid at 25 °C. In only 70 min, the ionogel disappeared, and a solution was obtained. The mechanism of the dissolution of the gel crosslinked by Schiff base bonds was found to be the hydrolysis of imine linkages in the presence of a lot of water.[30] Importantly, PAMAM dendrimer can easily precipitate from the above solution via the addition of acetone, and [EMIM][OAc] can be fully recycled and reused by distillation. This special property strongly enhances its environmental appeal.

Conclusions

In conclusion, we prepared novel self-healing ionogels with covalent polymeric networks based on PAMAM dendrimers by the in situ crosslinking of amines via Schiff base reaction in ionic liquids. The obtained ionogels have excellent self-healing and hydrolytic degradation properties. Oscillatory shear measurements indicate that the plateaus modulus in storage modulus increase with increasing PAMAM content, and increasing dendrimer generation decreases the plateaus modulus due to geometric constraints. Rheological investigation revealed that the ionogels are very stable, and the reversible covalent networks are not destroyed at temperatures up to 160 °C. Crucially, the ionogels exhibit high ionic conductivities exceeding 1.0×10^{-3} S cm^{-1}. Adding an appropriate amount of water to the ionogels results in a decrease in modulus but a sharp increase in ionic conductivity. The new ionogels are very promising for the preparation of high-performance gel polymer electrolytes for practical applications such as flexible electronic devices with self-healing properties.
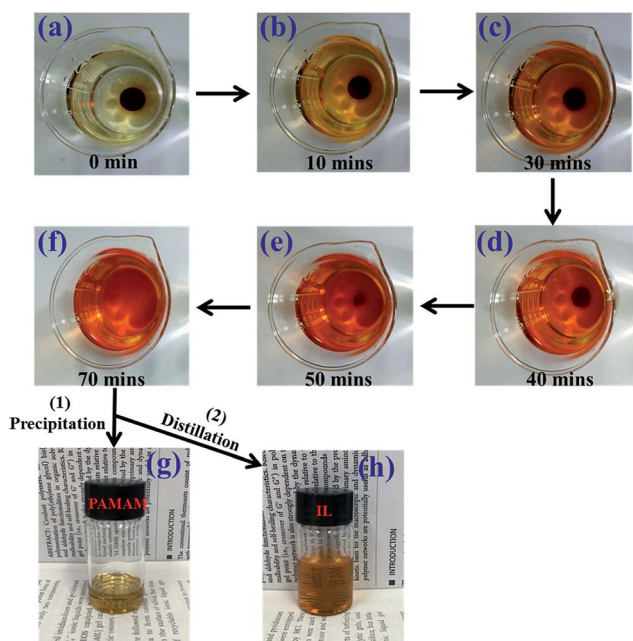
Acknowledgements

Fig. 7 Photographs showing the degradation and recycling process of the ionogel: (a)−(f) sample submerged in distilled water for different times; and (g) and (h) recycled PAMAM and ionic liquid.

References

1 T. P. Lodge, Science, 2008, 321, 50–51.

2 T. Ueki, R. Usui, Y. Kitazawa, T. P. Lodge and M. Y. Watanabe, *Macromolecules*, 2015, **48**, 5928–5933.

3 H. Srour, M. Leocmach, V. Maffeis, A. C. Ghogia, S. Denis-Quanquin, N. Taberlet, S. Manneville, C. Andraud, C. Bucher and C. Monnereau, *Polym. Chem.*, 2016, **7**, 6608–6616.

4 N. N. Zhao, Y. L. Liu, X. M. Zhao and H. Z. Song, *Nanoscale*, 2016, **8**, 1545–1554.

5 W. W. Xiong, H. L. Liu, Y. Z. Chen, M. L. Zheng, Y. Y. Zhao, X. B. Kong, Y. Wang, X. Q. Zhang, X. Y. Kong, P. F. Wang and L. Jiang, *Adv. Mater.*, 2016, **28**, 7167–7172.

6 T. Ueki, Y. Nakamura, R. Usui, Y. Kitazawa, S. So, T. P. Lodge and M. Watanabe, *Angew. Chem., Int. Ed.*, 2015, **54**, 3018–3022.

7 J. Le Bideau, L. Viau and A. Vioux, *Chem. Soc. Rev.*, 2011, **40**, 907–925.

8 T. Ueki and M. Watanabe, *Macromolecules*, 2008, **41**, 3739–3749.

9 C. S. Wei, M. M. Chen, D. Liu, W. M. Zhou, M. Khan, X. B. Wu, N. D. Huang and L. B. Li, *Polym. Chem.*, 2015, **6**, 4067–4070.

10 U. J. Kim, T. G. Kim, Y. Shim, Y. Park, C. W. Lee, T. H. Kim, H. S. Lee, D. Y. Chung, J. Kihm, Y. G. Roh, J. Lee, H. Son, S. Kim, J. Hur and S. W. Hwang, *ACS Nano*, 2015, **9**, 602–611.

11 M. D. Hager, P. Greil, C. Leyens, S. van der Zwaag and U. S. Schubert, *Adv. Mater.*, 2010, **22**, 5424–5430.

12 J. Hentschel, A. M. Kushner, J. Ziller and Z. Guan, *Angew. Chem., Int. Ed.*, 2012, **51**, 10561–10565.

13 P. Zhang and G. Li, *Prog. Polym. Sci.*, 2016, **57**, 32–63.

14 L. Schaedel, K. John, J. Gaillard, M. V. Nachury, L. Blanchoin and M. Thery, *Nat. Mater.*, 2015, **14**, 1156–1163.

15 K. Miyamae, M. Nakahata, Y. Takashima and A. Harada, *Angew. Chem., Int. Ed.*, 2015, **54**, 8984–8987.

16 C.-H. Li, C. Wang, C. Keplinger, J.-L. Zuo, L. Jin, Y. Sun, P. Zheng, Y. Cao, F. Lissel, C. Linder, X.-Z. You and Z. Bao, *Nat. Chem.*, 2016, **8**, 619–625.

17 I. Jeon, J. Cui, W. R. K. Illeperuma, J. Aizenberg and J. J. Vlassak, *Adv. Mater.*, 2016, **28**, 4678–4683.

18 T.-P. Huynh and H. Haick, *Adv. Mater.*, 2016, **28**, 138–143.

19 N. Annabi, S. R. Shin, A. Tamayol, M. Miscuglio, M. A. Bakooshli, A. Assmann, P. Mostafalu, J.-Y. Sun, S. Mithieux, L. Cheung, X. Tang, A. S. Weiss and A. Khademhosseini, *Adv. Mater.*, 2016, **28**, 40–49.

20 B. Zhu, N. Jasinski, A. Benitez, M. Noack, D. Park, A. S. Goldmann, C. Barner-Kowollik and A. Walther, *Angew. Chem., Int. Ed.*, 2015, **54**, 8653–8657.

21 D. Y. Wu, S. Meure and D. Solomon, *Prog. Polym. Sci.*, 2008, **33**, 479–522.

22 F. Herbst, D. Doehler, P. Michael and W. H. Binder, *Macromol. Rapid Commun.*, 2013, **34**, 203–220.

23 Y. Chen, A. M. Kushner, G. A. Williams and Z. Guan, *Nat. Chem.*, 2012, **4**, 467–472.

24 D. Y. Zhu, J. W. Guo, G. S. Cao, W. L. Qiu, M. Z. Rong and M. Q. Zhang, *J. Mater. Chem. A*, 2015, **3**, 1858–1862.

25 G. Deng, C. Tang, F. Li, H. Jiang and Y. Chen, *Macromolecules*, 2010, **43**, 1191–1194.

26 Y. Xin and J. Y. Yuan, *Polym. Chem.*, 2012, **3**, 3045–3055.

27 Y. Amamoto, H. Otsuka, A. Takahara and K. Matyjaszewski, *Adv. Mater.*, 2012, **24**, 3975–3980.

28 W. M. Xu, M. Z. Rong and M. Q. Zhang, *J. Mater. Chem. A*, 2016, **4**, 10683–10690.

29 Y. Jin, Q. Wang, P. Taynton and W. Zhang, *Acc. Chem. Res.*, 2014, **47**, 1575–1586.

30 A. Chao, J. Negulescu and D. Zhang, *Macromolecules*, 2016, **49**, 6277–6284.

31 G. Deng, F. Li, H. Yu, F. Liu, C. Liu, W. Sun, H. Jiang and Y. Chen, *ACS Macro Lett.*, 2012, **1**, 275–279.

32 Y. Zhao, Y. Zhang, H. Sun, X. Dong, J. Cao, L. Wang, Y. Xu, J. Ren, Y. Hwang, I. H. Son, X. Huang, Y. Wang and H. Peng, *Angew. Chem., Int. Ed.*, 2016, **55**, 14382–14386.

33 M. Zhang, D. Xu, X. Yan, J. Chen, S. Dong, B. Zheng and F. Huang, *Angew. Chem., Int. Ed.*, 2012, **51**, 7011–7015.

34 M. Nakahata, Y. Takashima, H. Yamaguchi and A. Harada, *Nat. Commun.*, 2011, **2**, 487–502.

35 D. C. Tuncaboylu, M. Sari, W. Oppermann and O. Okay, *Macromolecules*, 2011, **44**, 4997–5005.

36 S. Dong, B. Zheng, F. Wang and F. Huang, *Acc. Chem. Res.*, 2014, **47**, 1982–1994.

37 A. Harada, Y. Takashima and M. Nakahata, *Acc. Chem. Res.*, 2014, **47**, 2128–2140.

38 I. M. Van Meerbeek, B. C. Mac Murray, J. W. Kim, S. S. Robinson, P. X. Zou, M. N. Silberstein and R. F. Shepherd, *Adv. Mater.*, 2016, **28**, 2801–2806.

39 T. J. Trivedi, D. Bhattacharjya, J.-S. Yu and A. Kumar, *ChemSusChem*, 2015, **8**, 3294–3303.

40 M. Sharma, D. Mondal, C. Mukesh and K. Prasad, *Carbohydr. Polym.*, 2013, **98**, 1025–1030.

41 D. Astruc, E. Boisselier and C. Ornelas, *Chem. Rev.*, 2010, **110**, 1857–1959.

42 U. Boas and P. M. H. Heegaard, *Chem. Soc. Rev.*, 2004, **33**, 43–63.

43 M. Porus, F. Clerc, P. Maroni and M. Borkovec, *Macromolecules*, 2012, **45**, 3919–3927.

44 D. A. Tomalia, *Prog. Polym. Sci.*, 2005, **30**, 294–324.

45 W. Xu, P. A. Ledin, V. V. Shevchenko and V. V. Tsukruk, *ACS Appl. Mater. Interfaces*, 2015, **7**, 12570–12596.

46 J. F. Huang, H. M. Luo, C. D. Liang, I. W. Sun, G. A. Baker and S. Dai, *J. Am. Chem. Soc.*, 2005, **127**, 12784–12785.

47 W. Yang, J. Song, X. Wu, X. Wang, W. Liu, L. Qiu and W. Hao, *J. Mater. Chem. A*, 2015, **3**, 12154–12158.

48 J. R. McElhanon and D. R. Wheeler, *Org. Lett.*, 2001, **3**, 2681–2683.

49 M. L. Szalai, D. V. McGrath, D. R. Wheeler, T. Zifer and J. R. McElhanon, *Macromolecules*, 2007, **40**, 818–823.

50 Q. Wang, J. L. Mynar, M. Yoshida, E. Lee, M. Lee, K. Okuro, K. Kinbara and T. Aida, *Nature*, 2010, **463**, 339–343.

51 N. W. Polaske, D. V. McGrath and J. R. McElhanon, *Macromolecules*, 2010, **43**, 1270–1276.

52 K.-S. Krannig, D. Esposito and M. Antonietti, *Macromolecules*, 2014, **47**, 2350–2353.

53 P. K. Maiti, T. Cagin, G. F. Wang and W. A. Goddard, *Macromolecules*, 2004, **37**, 6236–6254.

54 Q. Wei, J. Wang, X. Shen, X. A. Zhang, J. Z. Sun, A. Qin and B. Z. Tang, *Sci. Rep.*, 2013, **3**, 1093.

55 S. Zhang, K. H. Lee, C. D. Frisbie and T. P. Lodge, *Macromolecules*, 2011, **44**, 940–949.

56 S. Zhang, K. H. Lee, J. Sun, C. D. Frisbie and T. P. Lodge, *Macromolecules*, 2011, **44**, 8981–8989.

57 T. Kakuta, Y. Takashima, M. Nakahata, M. Otsubo, H. Yamaguchi and A. Harada, *Adv. Mater.*, 2013, **25**, 2849–2853.

58 Y.-L. Rao, A. Chortos, R. Pfattner, F. Lissel, Y.-C. Chiu, V. Feig, J. Xu, T. Kurosawa, X. Gu, C. Wang, M. He, J. W. Chung and Z. Bao, *J. Am. Chem. Soc.*, 2016, **138**, 6020–6027.

59 E. Borre, J.-F. Stumbe, S. Bellemin-Laponnaz and M. Mauro, *Angew. Chem., Int. Ed.*, 2016, **55**, 1313–1317.

60 D. Doehler, P. Zare and W. H. Binder, *Polym. Chem.*, 2014, **5**, 992–1000.

61 W. J. Li, Z. F. Zhang, B. X. Han, S. Q. Hu, Y. Xie and G. Y. Yang, *J. Phys. Chem. B*, 2007, **111**, 6452–6456.

62 M. L. P. Le, L. Cointeaux, P. Strobel, J. C. Lepretre, P. Judeinstein and F. Alloin, *J. Phys. Chem. C*, 2012, **116**, 7712–7718.

63 X. H. Liu, D. B. Wu, H. L. Wang and Q. G. Wang, *Adv. Mater.*, 2014, **26**, 4370–4375.

64 I. McCulloch, M. Heeney, C. Bailey, K. Genevicius, I. MacDonald, M. Shkunov, S. Sparrowe, S. Tierney, R. Wagner, W. Zhang, M. L. Chabinyc, R. J. Kline, M. D. McGehee and M. F. Toney, *Nat. Mater.*, 2006, **5**, 328–333.

65 B. Tang, S. P. White, C. D. Frisbie and T. P. Lodge, *Macromolecules*, 2015, **48**, 4942–4950.